Double Stern-Gerlach experiments on $Mn@Sn_{12}$: Refocusing of a paramagnetic superatom

Thomas M. Fuchs* and Rolf Schäfer

Eduard-Zintl-Institut für Physikalische und Anorganische Chemie, Technische Universität Darmstadt, Alarich-Weiss-Straße 8, 64287 Darmstadt, Germany

(Received 28 September 2018; published 11 December 2018)

We report magnetic double deflection experiments on cryogenically cooled $Mn@Sn_{12}$ clusters. Refocusing efficiencies of up to 90% are achieved by keeping the magnetic-flux density virtually constant between the two Stern-Gerlach magnets. The spin dynamics are probed by introducing magnetic-flux density variations along the molecular-beam path. We apply a microscopic model for the interpretation of our results taking the coupling of electronic spin and rotational degrees of freedom into account. The combination of our experimental and theoretical results reveals unexpected insights into the interplay between rotation and spin dynamics of small metal clusters depending on magnetic-field modulations.

DOI: 10.1103/PhysRevA.98.063411

I. INTRODUCTION

The question of how spin relaxation may occur in isolated, small, and vibrationally cold clusters and molecules is a long-standing fundamental problem in cluster science. First evidence for spin relaxation in collision-free molecular beams was found in (double) Stern-Gerlach experiments on molecules [1,2] and small alkali-metal clusters [3,4]. A significant fraction of the molecular beam was found to be hardly deflected in contradiction to the expected space quantization in atoms and small molecules.

Starting in the early 1990s magnetic properties of transition-metal clusters have been studied in Stern-Gerlach experiments [5–25]. Iron, nickel, and cobalt clusters in the size range from ten up to a few hundred atoms were exclusively deflected in the direction of the magnetic-field gradient which implies some kind of spin relaxation and orientation inside the magnetic field. When highly vibrationally excited, the experimental results were in good agreement with the Langevin model assuming that the clusters are in contact with some kind of internal heat bath. For very small clusters in cryogenically cooled molecular beams (down to 20 K) this is not a good assumption and indeed, significant deviations from this simple statistical approach were found and discussed for almost 20 years [8,14,15,18,22,23]. A reasonable model was presented for bare cobalt clusters by Xu *et al.* explicitly taking the repulsion between adiabatic states in the rotation-Zeeman diagram into account [21,24]. This proposed avoided-crossing model converges to the Langevin model in the high-temperature limit and will be discussed in detail and utilized for our purposes.

Our work focuses on alloy clusters consisting of nonmagnetic elements doped with one atom that carries a magnetic moment [26–28]. These are the most simple cluster species for investigations of their magnetic behavior since no spin-spin coupling can occur. However, the size and geometry dependence of experimental observations have not been completely understood until today. For most cluster species a uniform deflection in the gradient direction was observed for all experimental conditions. This is in accordance with previous Stern-Gerlach experiments on larger transition-metal clusters. However, for the cold icosahedral cage-cluster $Mn@Sn_{12}$ an atomlike equidistant splitting in six beamlets was found corresponding to space quantization with total electronic angular momentum quantum number $J = 5/2$ [26]. Obviously, the spin state of this so-called superatomic cluster is preserved inside the magnet while some other alloyed cluster species also showed at least a partial atomlike deflection behavior. These observations raise some questions: (i) Is it possible to reverse the molecular-beam splitting with a second Stern-Gerlach magnet, i.e., to refocus the cluster beam? (ii) Is the spin state still conserved when the magnetic-flux density changes rapidly? In the following, these issues shall be addressed in detail.

Our long-term goal is to perform molecular-beam magnetic resonance (MBMR) experiments on atomlike clusters [29]. The magnetic refocusing in a double Stern-Gerlach experiment is a key step going from pure deflection to magnetic-resonance experiments. Additionally, refocusing experiments reveal interesting details on spin dynamics of the studied species in time-varying fields and are therefore sensitive to spin-rotation coupling.

II. EXPERIMENTAL DETAILS

A detailed description of our molecular-beam deflection apparatus has been reported before [27,30]. Briefly, neutral metal clusters are produced by pulsed laser vaporization of a Mn-Sn target rod (5 mol% Mn in Sn) with a frequency doubled Nd:YAG laser (532 nm) in a pulsed helium gas flow. A pure Bi target for the generation of an atomic Bi beam has been used for calibration and comparison. The helium-cluster mixture is thermalized in a cryogenically cooled, temperature-controlled nozzle. The nozzle can be cooled down to $T_{\text{nozzle}} \geqslant 16$ K. Previous investigations proved that the clusters are well thermalized and vibrational temperatures coincide well

*fuchs@cluster.pc.chemie.tu-darmstadt.de

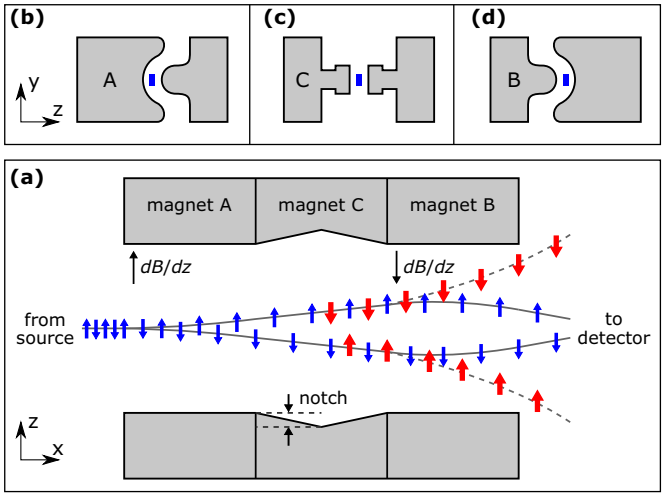

FIG. 1. (a) Schematic diagram of the magnet arrangement in the refocusing experiment and representative trajectories for spin-1/2 particles. Arrows symbolize the spin orientation. An unpolarized beam of cold clusters emerges from the cluster source. Magnets A and B produce inhomogeneous fields with antiparallel field gradient while the direction of the magnetic flux B is oriented in the same direction. Particles that change their spin orientation in the C magnet are highlighted with bold, red arrows. The pole shoe distance in z direction is greatly exaggerated. Panels (b)–(d) show the pole shoe geometries parallel to the molecular-beam direction.

with T_{nozzle} for expansion conditions above $T_{\text{nozzle}} = 30$ K [26,27,31,32]. For lower T_{nozzle} thermalization is incomplete, probably due to an insufficient dwell time [26,33]. After expansion of the helium-cluster mixture into high vacuum a molecular beam is formed which is shaped by two conical skimmers and further collimated to a rectangular shape by two slits. Subsequently, the molecular beam passes the deflection region. The magnet setup was modified for the experiments that are presented in this work, therefore it is described in more detail here.

Figure 1(a) shows particle trajectories for species with $J = 1/2$ within the magnetic refocusing arrangement assuming that changes of the spin state only occur in the region of magnet C. The unpolarized clusters enter the first inhomogeneous magnetic field A where beams of atoms and atomlike clusters equidistantly split in $2J + 1$ components. All particles that retain their spin state (blue arrows) are refocused in the second inhomogeneous field as the field gradient B is aligned antiparallel referring to field A. Spin flips in the C magnet lead to defocusing (bold, red arrows) and thus a reduction of intensity on the molecular-beam axis.

The magnetic fields are generated by a single, home-built electromagnet with three consecutive, interchangeable pole shoe pieces. For inhomogeneous fields the two-wire geometry [34] shown in Figs. 1(b) and 1(d) (0–1.3 T, 0–355 T m^{-1}) is used. The magnetic-flux density is measured with a Hall probe. The field gradient is calibrated by Stern-Gerlach experiments on the bismuth atom [26,35]. The homogeneous field in magnet C is generated by flat pole shoes which are designed to produce the same magnetic-flux density on the molecular-beam path like the two-wire pole shoes. When the pole shoe gap becomes larger by introducing a notch depicted in Fig. 1(a), the magnetic-flux density on the molecular-beam path decreases from its maximum value $B_A = 1.3$ T inside the inhomogeneous field of magnet A to $B_{\text{C,min}} = 0$–1.2 T depending on the notch and then increases to $B_B = 1.3$ T again.

After passing the deflection and drift regions, the clusters are photoionized and detected by time-of-flight mass spectrometry. The beam profiles are scanned by translating a slit across the molecular beam in the z direction.

III. REFOCUSING EXPERIMENTS

Refocusing efficiencies are extracted from a fit to the experimental data. It is assumed that the probability for a spin flip p_{flip} in magnet C does not depend on the initial and finale spin state. It is further assumed that the magnetic spin states are initially uniformly distributed while spin flips only occur in magnet C between A and B. The probability for the spin state in magnet A being equal to the projection M_J^A and the spin state in magnet B being equal to M_J^B is given by $P_{M_J^A M_J^B}$. When no spin flips occur ($p_{\text{flip}} = 0$), diagonal elements in $P_{M_J^A M_J^B}$ have the value $1/(2J + 1)$ and off-diagonal elements vanish. When the spin of practically all particles flips ($p_{\text{flip}} = 1$), M_J^B is independent of M_J^A. Thus, all elements of $P_{M_J^A M_J^B}$ are given by $1/(2J + 1)^2$. Between these limiting cases one finds

$$P_{M_J^A M_J^B} = \frac{p_{\text{flip}}}{(2J+1)^2} + \delta_{M_J^A M_J^B} \frac{(1 - p_{\text{flip}})}{2J+1}. \tag{1}$$

Molecular-beam intensity profiles with magnetic field ϕ_{on} were calculated from the profiles without field ϕ_{off} according to

$$\phi_{\text{on}}(z) = \sum_{M_J^A} \sum_{M_J^B} P_{M_J^A M_J^B} \phi_{\text{off}}\left(z - d_{M_J^A M_J^B}\right) \tag{2}$$

with

$$d_{M_J^A M_J^B} = \frac{\mu_B g_J}{m v_x^2} \left[\gamma_A \left(\frac{dB}{dz}\right)_A M_J^A + \gamma_B \left(\frac{dB}{dz}\right)_B M_J^B \right]. \tag{3}$$

The constants γ_A and γ_B depend only on the apparatus dimensions [27]. The parameters $d_{M_J^A M_J^B}$, v_x, m, and dB/dz, are the deflection, cluster velocity, mass, and field gradient, respectively. The Landé factor is assumed to be equal to the pure spin value of $g_J = 2$ for Mn@Sn$_{12}$ and $g_J = 1.65$ with $J = 3/2$ for the Bi atom [35].

Only particles with the same spin state in magnets A and B are refocused. Therefore, the refocusing efficiency is defined by

$$\eta_{\text{refoc}} = \sum_{M_J} P_{M_J M_J} = 1 - \frac{2J}{2J+1} p_{\text{flip}}. \tag{4}$$

Thus, η_{refoc} is the probability for a cluster to remain in the same spin state or in other words, to not undergo a spin flip. The smallest possible refocusing in this model is $1/(2J + 1)$ for $p_{\text{flip}} = 1$ and it occurs when M_J^B is completely independent of M_J^A. The probability p_{flip} was extracted from the experiment by fitting Eq. (2) with p_{flip} being the only adjustable parameter to the experimental beam profiles. Plugging the result in Eq. (4) gives the experimental refocusing efficiency.

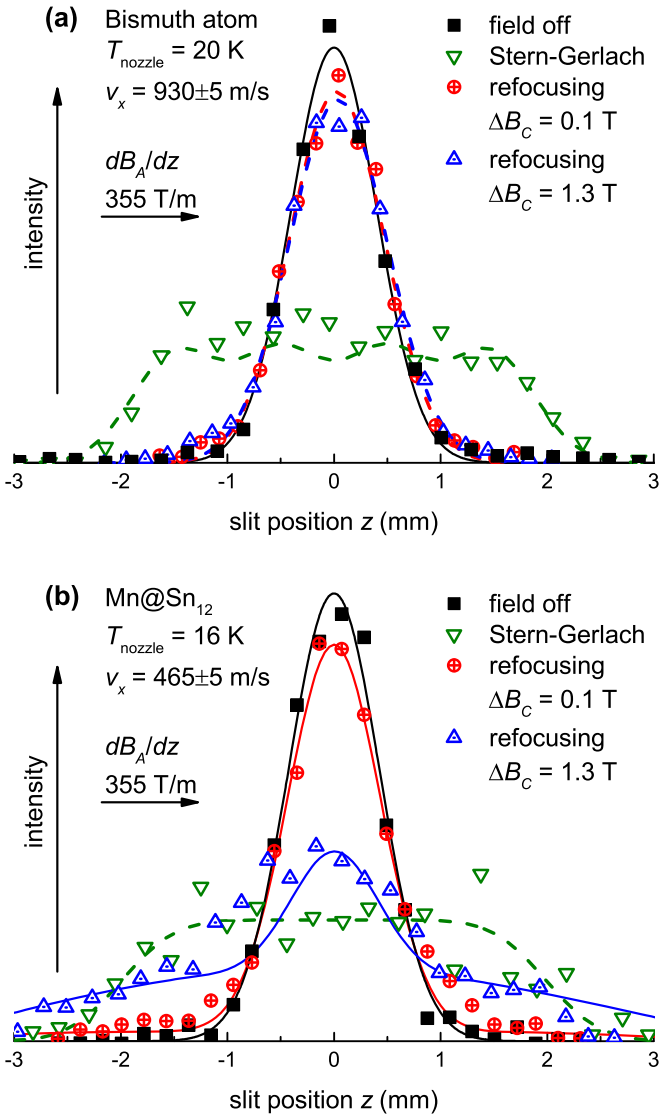

FIG. 2. Results from Stern-Gerlach and refocusing experiments for the bismuth atom (a) and the $Mn@Sn_{12}$ cluster (b). The black and all dashed lines are Gauss fits (Stern-Gerlach profiles: $2J+1$ equidistant Gaussian components), the lines for both refocusing experiments on $Mn@Sn_{12}$ are results from calculations employing the avoided-crossing model described in Sec. IV ($p_{ad} = 1.5\%$).

Figure 2 shows the beam profiles for Stern-Gerlach and refocusing experiments of the (a) bismuth atom and (b) $Mn@Sn_{12}$. Stern-Gerlach beam profiles (green triangles) were measured using one pair of pole shoes in magnet A (length: 45 mm). A plateau instead of a splitting was observed because the $2J+1$ components are not resolved due to the small length of the magnet. Increasing the length of the inhomogeneous field leads to a splitting in four and six components for the bismuth atom and $Mn@Sn_{12}$, respectively [26].

For refocusing experiments (red dots in Fig. 2) two Stern-Gerlach magnets A and B with antiparallel field gradients were used, like depicted in Fig. 1. In between, flat pole pieces (magnet C, no notch) were installed to hold the magnetic-flux density constant along the molecular beam within ±0.1 T over the whole length of the magnet. For the bismuth atom as well as the $Mn@Sn_{12}$ cluster, only a small intensity drop in the center of the molecular-beam profile was observed. Applying Eq. (2) to the beam profiles, values for $p_{flip} \approx 0.1$ were obtained, i.e., η_{refoc} was better than 90% in both cases. The beam profiles are slightly asymmetric which will be discussed in Appendix A in more detail. In the following, the magnetic-flux density drop in between the two inhomogeneous magnetic fields was gradually increased by adding a notch to the C magnet as depicted in Fig. 1(a). Ultimately, the pole pieces of magnet C were removed completely. In this case $B_{C,min}$ was on the order of a few millitesla, i.e., the change of the flux density in region C is $\Delta B_C = B_A - B_{C,min} = 1.3$ T (blue triangles in Fig. 2). For the bismuth atom, refocusing better than 90% was still observed under these experimental conditions. In contrast, the beam profile of $Mn@Sn_{12}$ is considerably broadened and the intensity at the beam center is only slightly increased compared to the corresponding Stern-Gerlach experiment. Again applying Eq. (2) gives $p_{flip} \approx 0.78$, i.e., η_{refoc} is about 35%. These experimental observations imply that transitions between the different spin states of $Mn@Sn_{12}$ must have occurred in the gap between the two Stern-Gerlach magnets. This experiment was performed for different notch depths to vary the change of the magnetic-flux density ΔB_C and therefore its rate dB_C/dt. These results will be presented after a brief discussion of the avoided-crossing model.

IV. AVOIDED-CROSSING MODEL

In order to explain the experimental results, a microscopic model based on the avoided-crossing theory described by de Heer and co-workers [21,24] is applied. For the cluster thermalization conditions in this work ($T_{nozzle} = 16$ K), $Mn@Sn_{12}$ clusters are in their electronic and vibrational ground state [26]. Figure 3 shows the rotational and spin eigenstates (rotation-Zeeman diagram) for the spherical rotor $Mn@Sn_{12}$ taking the thermally accessible energy levels for a typical rotational temperature of $T_{rot} = 10$ K into account [27].

For the construction of the rotation-Zeeman diagram, the coupling of spin and rotational degrees of freedom has to be considered. Spin-rotation coupling arises from zero-field splittings (ZFSs) of the spin microstates [27]. Consequently, level crossings are avoided when the total angular momentum quantum number in the field direction $J_z^{tot} = R_z + M_J$ containing contributions from rotation (R_z) and spin (M_J) is conserved. For clarity, the uppermost graph in Fig. 3 shows two crossing energy levels for which angular momentum conservation holds. When the levels are not coupled they simply follow the uncoupled states (grey lines); the spin state does not change. However, for the coupled case the level crossing is avoided. It now depends on the magnitude of the spin-rotation coupling Δ_{SR} and the rate of the change of magnetic-flux density dB/dt how these states evolve during the crossing: Large couplings and slow field changes favor an adiabatic passage (dashed, green line) and thus a change of the spin state. For small Δ_{SR} and large dB/dt, the probability for a diabatic traverse of the avoided level crossing following the uncoupled states is increased.

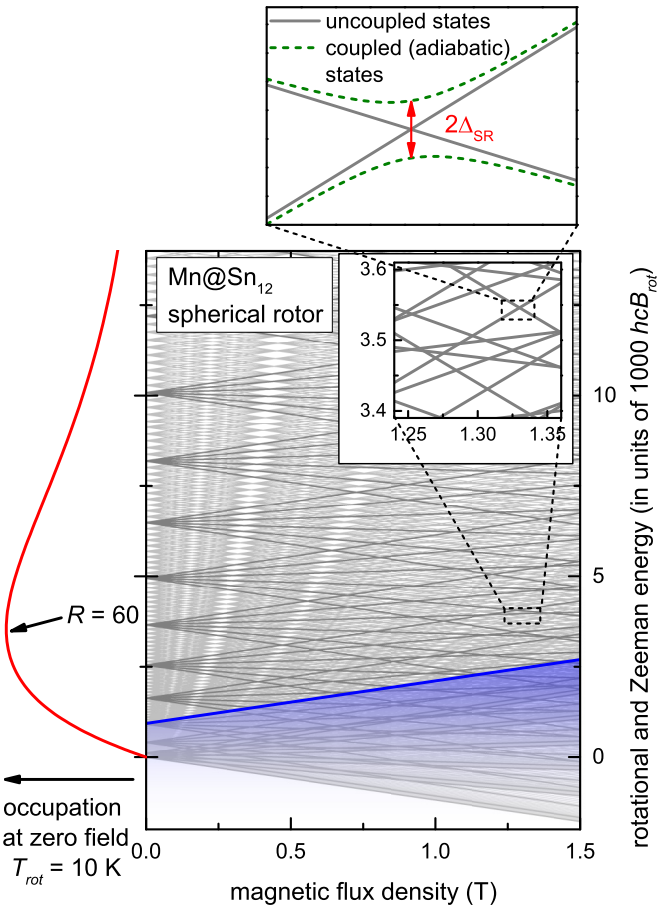

FIG. 3. Rotation-Zeeman diagram for Mn@Sn$_{12}$ (spherical rotor with $B_{\rm rot} = 0.2\,{\rm m}^{-1}$) [27]. The energy levels with rotational quantum number $R = 0, 10, 20, \ldots$ are highlighted in dark grey for a better overview. The inset shows the level crossing density around the magnetic-flux density in the Stern-Gerlach magnets and the upper graph is zoomed in to one of these level crossings. The energy state with $M_J = 2.5$ and $R = 30$ is highlighted (bold, blue). There is no energy level with $M_J = 2.5$ below this curve that could interact with states having $J_z^{\rm tot} = R_z + M_J = 32.5$ because of $|M_J| \leqslant J$ and $|R_z| \leqslant R$ (see text for further details). The red curve on the left side shows the Boltzmann distribution for the rotational levels at zero field.

A. Qualitative considerations

The magnetic field along the particle trajectory in magnet A varies on the order of a few tens of millitesla [27] due to the deflection during the passage of the inhomogeneous field. The observed deflection in Stern-Gerlach experiments is at least proportional to the time average of the magnetic moment in the gradient direction $\langle \mu_z \rangle$ inside the magnet. It has been shown that for pure cobalt clusters molecular-beam deflection and broadening effects in Stern-Gerlach experiments can be understood taking the average slope and the density of level crossings in the Rotation-Zeeman diagram into account [21,24].

For the icosahedral cage cluster Mn@Sn$_{12}$ the ZFS vanishes. Therefore, spin-rotation coupling can be neglected to first order and level crossings are not avoided. In this case, all clusters would follow the uncoupled energy levels and no spin flips occur. Consequently, a splitting of the molecular beam in Stern-Gerlach experiments at low temperatures is observed. The number of level crossings due to the deflection can be estimated as follows: In our earlier Stern-Gerlach experiments with a magnet A of 80 mm length [26] Mn@Sn$_{12}$ clusters are deflected about 60 μm on average inside the magnet which corresponds to a change in magnetic-flux density of about $\Delta B_A = 20$ mT. The average level spacing for the rotational quantum number $R = 60$ (largest occupation at $T_{\rm rot} = 10$ K) at 1.3 T is also about $\Delta B_{\rm cross} = 20$ mT. In fact, ΔB_A will be larger due to slight misalignments of the magnet setup. The average number of level crossings is then expected to be at least close to 1. Even a single spin flip would suppress the equidistant splitting of the molecular beam [27]. Therefore, one has to conclude from these considerations that most level crossings inside the magnet are traversed diabatically, i.e., the clusters follow the uncoupled states.

However, the breakdown of $\eta_{\rm refoc}$ for increasing flux density changes in the refocusing experiments must be due to spin flips and therefore some level crossings are actually avoided, i.e., a small spin-rotation coupling $\Delta_{\rm SR} \neq 0$ must be present in the Mn@Sn$_{12}$ cluster. At an avoided level crossing in a two-level system the diabatic transition probability $p_{\rm LZ}$ can be analytically expressed by the Landau-Zener formula

$$p_{\rm LZ} = 1 - p_{\rm ad} = \exp\left(-\frac{2\pi\,\Delta_{\rm SR}^2}{\mu_{\rm B} h |M_J - M_J'| dB/dt}\right) \qquad (5)$$

with dB/dt being the velocity for going through the crossing point [24,36]; $p_{\rm ad}$ is the probability for the adiabatic case, and M_J and M_J' are the spin states before and after the crossing, respectively.

The spin-rotation coupling $\Delta_{\rm SR}$ responsible for the avoided crossings arises from several mechanisms. For the pure spin magnetism of Mn@Sn$_{12}$ with $J = S = 5/2$, spin-orbit coupling can be neglected in a first approach. Therefore, the coupling of a rotating charge distribution with a magnetic dipole moment should be the most important contribution. Taking the average angular frequency ω of the cluster rotation with $\frac{2}{5} m r^2 \omega^2 = 3 k_B T_{\rm rot}$ into account and approximating the cluster radius r with the Wigner-Seitz radius of tin one finds [24]

$$\Delta_{\rm SR} \approx \frac{\mu \mu_0 e \omega}{r} \approx 8 \times 10^{-9}\ {\rm eV} \qquad (6)$$

for Mn@Sn$_{12}$ with $\mu = g_J \sqrt{J(J+1)}\mu_{\rm B} \approx 5.9 \mu_{\rm B}$ at $T_{\rm rot} = 10$ K. Inserting this value in Eq. (5) taking a typical rate of magnetic-flux density change $dB_A/dt = 100\ {\rm T\,s}^{-1}$ inside magnet A in a Stern-Gerlach experiment into account gives $p_{\rm LZ} \approx 0$. Thus, practically all avoided level crossings should be traversed adiabatically which means that the spin state of the cluster changes at every single avoided level crossing. The observations in Stern-Gerlach experiments contradict this qualitative estimation: A splitting of the molecular beam in $2J + 1$ components is observed experimentally which implies that there are practically no spin flips inside the magnetic field.

In order to resolve the discrepancy between experimental results and qualitative arguments within the two-state Landau-Zener model, the spin dynamics at level crossings in the Rotation-Zeeman diagram will be discussed in more detail.

B. Quantitative considerations

In the following, an approach to calculate refocusing efficiencies and molecular-beam profiles based on the avoided-crossing model is described stepwise. Thereby, possible trajectories through the rotation-Zeeman diagram are explicitly considered, taking adiabatic or diabatic level crossings into account. Running 50 000 separate calculations considering one cluster each, the standard deviation of the refocusing efficiency and the intensity in the calculated molecular-beam profiles becomes smaller than the experimental uncertainty.

1. Cluster generation, field entrance, and exit

In our molecular-beam apparatus, clusters are produced at zero field. Thus, in the first step the rotational energy levels are populated using a Boltzmann distribution for a typical rotational temperature of 10 K (red curve in Fig. 3) [27]. The $2J+1$ spin states are assumed to be uniformly occupied in the cluster source at zero field.

When clusters enter the first inhomogeneous field A, the magnetic-flux density increases from 0 to 1.3 T and a large number of level crossings is traversed. It is not trivial to decide from experimental observations and calculations whether these crossings are traversed adiabatically or diabatically. In any case, adiabatic level crossings lead to a slight imbalance in the spin-state population. Nevertheless, the effect on refocusing experiments for our experimental conditions is small. Therefore, it is reasonable to assume an equal distribution of the spin states after field entrance for the following steps. However, this issue will be discussed in more detail in Appendix B.

In analogy to the field entrance, clusters traverse a large number of level crossings when the flux density drops from about 1.3 T to zero when they exit magnet B. Since no deflection fields follow, spin flips occurring here do not affect the deflection or refocusing experiments. Therefore, the field exit is not considered in our calculations.

2. Refocusing

After field entrance, the clusters traverse magnet A. From Stern-Gerlach experiments we know that the spin state must be preserved. Therefore, the small change of the magnetic-flux density (a few millitesla) due to the deflection inside the magnetic field can be safely neglected. The same assumption is applied to the inhomogeneous field B. Thus, the calculated molecular-beam profiles depend only on the spin flips occurring in section C between the inhomogeneous fields. Every run in the calculation is started from the energy level in the rotation-Zeeman diagram after the field entrance at $B_A = 1.3$ T and explicitly goes through all level crossings down to $B_{C,\min} = 0 - 1.2$ T (Fig. 4). Either a constant probability for an adiabatic passage at avoided level crossings or the two-state Landau-Zener probability according to Eq. (5) is applied. The change rate of the magnetic-flux density dB_C/dt is assumed to be constant. Subsequently, these steps are repeated from the value of $B_{C,\min}$ to $B_B = 1.3$ T. Molecular-beam profiles and η_{refoc} are calculated using Eqs. (2) and (4), respectively. Here, $P_{M_J^A M_J^B}$ is taken from the 50 000 calculation runs. The calculated refocusing efficiency is compared to the experimental

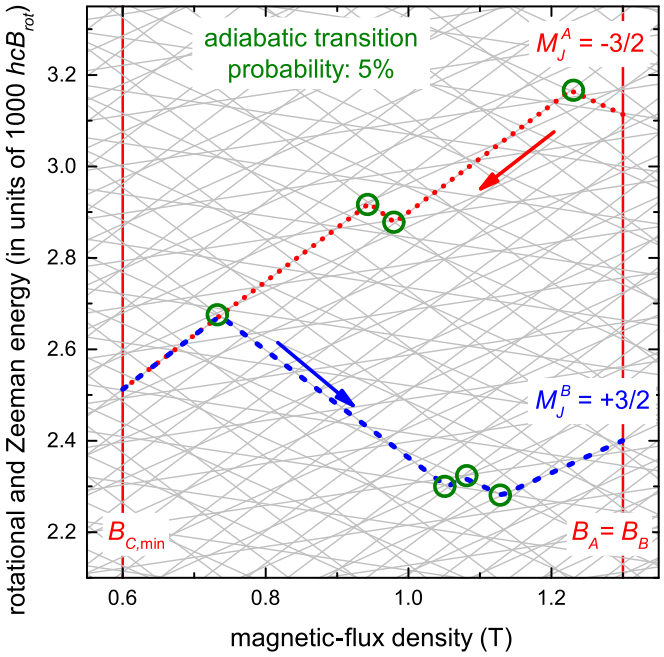

FIG. 4. Exemplary paths through the rotation-Zeeman diagram depicting one calculation run for the transition region C between the inhomogeneous fields in the refocusing experiment. The magnetic-flux density in fields A and B is $B_A = B_B = 1.3$ T, the minimum flux density in magnet C is given by exemplary $B_{C,\min} = 0.6$ T. Starting from B_A at the energy level after field entrance the level crossings are traced down to $B_{C,\min}$ (red, dotted line). Avoided level crossings are traversed adiabatically with a probability of 5%. An adiabatic passage is indicated by a green circle. This procedure is repeated from $B_{C,\min}$ back to B_B (blue, dashed line).

behavior for values of $\Delta B_C = 0.1$ to 1.3 T in Fig. 5. Beam profiles calculated with Eq. (2) are shown in Fig. 2(b) ($p_{\text{ad}} = 1.5\%$). The best agreement with the experimental results is found for a constant adiabatic transition probability $p_{\text{ad}} = (1.0\text{–}1.5)\%$ at every avoided level crossing.

Applying the two-state Landau-Zener formula in Eq. (5), the calculated refocusing efficiency hardly varies with ΔB_C (red, dotted symbols in Fig. 5). The spin-rotation coupling can be chosen to reproduce at least the magnitude of η_{refoc}, if Δ_{SR} is in the range of 10^{-9} eV which agrees with the qualitative estimation in Eq. (6). The number of traversed level crossings increases approximately linearly with ΔB_C but the probability for a spin to actually flip at one of the crossings p_{ad} decreases due to a larger value of dB_C/dt. These effects compensate each other in the limiting case when the exponent in Eq. (5) is small (i.e., for small Δ_{SR}) thus leading to a nearly constant value for η_{refoc}. However, even for larger values of Δ_{SR} the calculations based on the Landau-Zener model clearly contradict the experimental trends.

C. Atom vs superatomic cluster

The avoided-crossing theory fits the experimental results for $Mn@Sn_{12}$ clusters well for a constant value of $p_{\text{ad}} = (1.0\text{–}1.5)\%$. Referring to Fig. 2(a) it was observed that the bismuth atom is refocused even when the magnetic-flux density drops to almost zero between magnets A and B. This

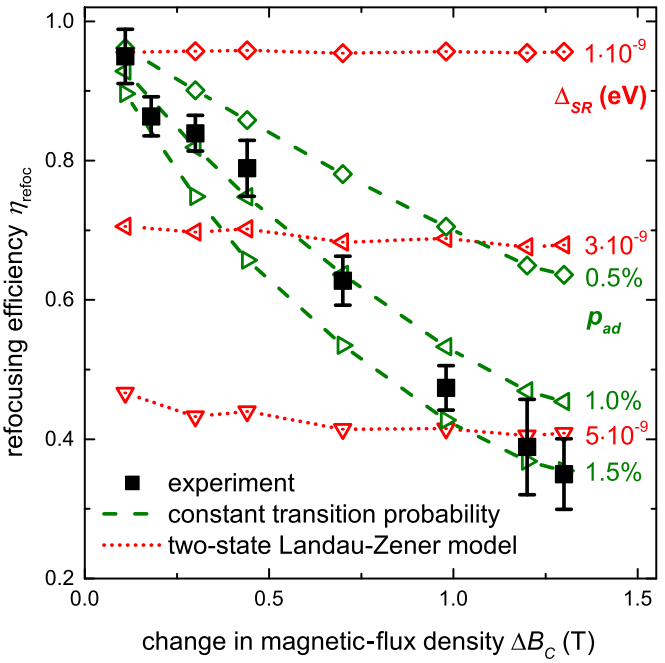

FIG. 5. Refocusing efficiency η_{refoc} according to Eq. (4) in dependence of the magnetic-flux density change in magnet C. The experimental values (black squares) are determined by fitting Eq. (2) to the measured beam profiles. Simulations with a constant probability for an adiabatic crossing (p_{ad}, green hollow symbols) and the two-state Landau-Zener transition probability according to Eq. (5) with spin-rotation coupling constant Δ_{SR} (red, dotted symbols) are shown. For the latter, dB_C/dt is assumed to be constant within magnet C, i.e., $\Delta B_C \propto dB_C/dt$.

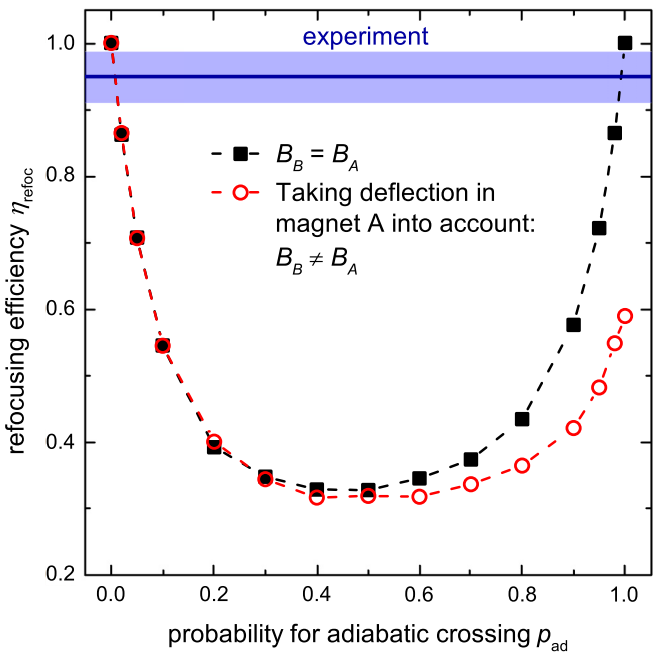

FIG. 6. Calculated refocusing efficiency from $p_{\text{ad}} = 0$ (fully diabatic) to 1 (fully adiabatic). B_A and B_B are the magnetic-flux densities on the cluster trajectory in magnets A and B, respectively. All parameters were chosen to represent the refocusing experiment with the lowest change in the magnetic-flux density ($\Delta B_C = 0.11$ T). The blue line is η_{refoc} from the experimental data and the shaded area its error range.

experimental observation is in line with our considerations: Atoms have no rotational degrees of freedom and thus, there are no level crossings that could induce spin flips. It has already been shown in the 1930s that in order to change the spin orientation of atoms one needs weak and rapidly varying (rotating) fields, such that field rotation and Larmor precessions are on the same time scale [37]. This concept leads directly to the magnetic-resonance method developed by Rabi and co-workers [29]. Therefore, the spin state of the bismuth atom is not influenced by the change of the magnetic-flux density ΔB_C in our refocusing experiments.

V. DISCUSSION

Rather small adiabatic transition probabilities of about $p_{\text{ad}} \approx (1.0\text{–}1.5)\%$ fit the experimental data best. In other words, the majority of avoided level crossings is diabatic. In principle, refocusing can occur in both limits; it is only important that clusters follow the same path in the rotation-Zeeman diagram out of magnet A and into magnet B [4]. This means that the refocusing efficiency for $p_{\text{ad}} = 0.99$ is comparable to $p_{\text{ad}} = 0.01$ as long as the magnetic flux densities in magnets A and B are assumed to be equal. However, the deflection of a few tens of micrometers from magnet A to B alone leads to a difference in the magnetic-flux density $\Delta B_{\text{A-B}} = B_A - B_B$ on the molecular beam path of at least a few tens of millitesla, ignoring any misalignments that further increase $\Delta B_{\text{A-B}}$. This shift is significant as it is in the same range or even larger than the spacing between two level crossings (compare Fig. 3, inset). Therefore, Fig. 6 shows the calculated refocusing efficiency for Mn@Sn$_{12}$ for $\Delta B_C = 0.1$ T [corresponding experiment: red dots in Fig. 2(b)] for different constant adiabatic transition probabilities taking the shift $\Delta B_{\text{A-B}}$ into account. For small p_{ad} the magnetic-flux density shift has no significant effect on the refocusing efficiency since there are no spin flips at the majority of avoided crossings and thus a small variation of the number of crossings is not significant. However, for $p_{\text{ad}} > 0.5$ significantly reduced refocusing efficiencies are calculated taking ΔB_{A-B} into account; even for $p_{\text{ad}} = 1$ the refocusing efficiency is only 60%. However, in the experiments, refocusing efficiencies of about 90% were observed. Thus, within the proposed model, only $p_{\text{ad}} \ll 1$ can explain the experimental results. Additionally, this is qualitatively in line with the consideration of the level-crossing density in Stern-Gerlach experiments in Sec. IV A.

In order to further validate values of $p_{\text{ad}} \ll 1$ the magnetic field (and thus its gradient) in magnet B was varied independently from A. Two separate Stern-Gerlach magnets bridged with a homogeneous field produced by permanent magnets were used for this experiment and the intensity on the molecular beam axis after refocusing was measured. One would expect a rather broad maximum of the refocusing efficiency for the mainly diabatic case because the spin state rarely changes and consequently, small flux density differences between the inhomogeneous fields are not significant. For the adiabatic case, efficient refocusing only occurs when the magnetic-flux

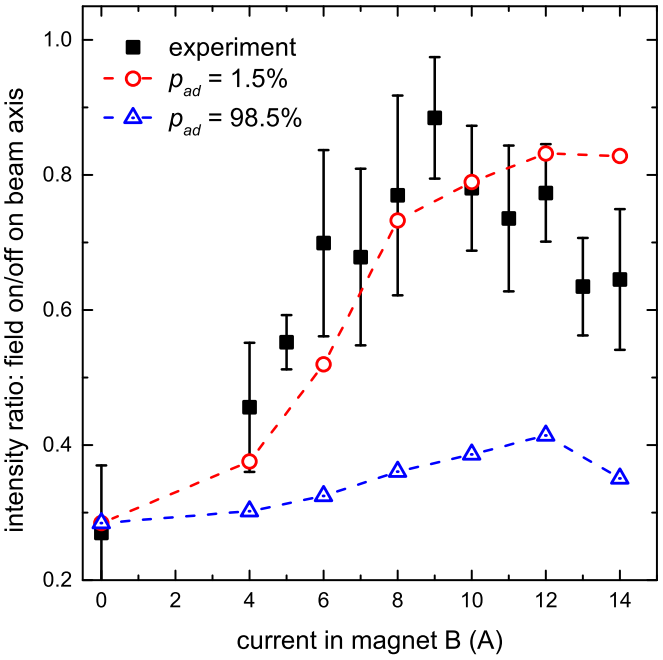

FIG. 7. Intensity of $Mn@Sn_{12}$ on the molecular-beam axis for different currents and thus magnetic-flux densities and field gradients in magnet B. Calculations were performed in the diabatic and adiabatic limiting case. All parameters were equal to the experiments shown in Fig. 2 except the length of the magnetic-field sections is larger here. The lowest observed intensity on the molecular-beam axis is around 27% of the intensity without magnetic fields and is due to an incomplete splitting of the molecular beam in the first Stern-Gerlach magnet.

density in magnets A and B differs by less than the average spacing between avoided level crossings. One would therefore expect a sharp maximum around $B_A = B_B$. However, due to the deflection from magnet A to magnet B and ubiquitous, slight misalignments, the magnetic-flux density on the beam path will always vary by a few tens of millitesla or more in our experiments. Thus, the expected maximum of η_{refoc} in the adiabatic case is blurred. In fact, the calculated results (blue triangles in Fig. 7) do not fit the experimental data at all. The diabatic case in Fig. 7 qualitatively agrees with the experiment. However, the drop of refocusing efficiency for large currents in magnet B indicates an over-refocusing of the molecular beam that is not explained by our calculations. This could be due to the small dependence of the field gradient on the z position which causes (de)focusing effects in Stern-Gerlach experiments.

The question remains why a constant adiabatic transition probability of about 1% at every avoided level crossing explains the refocusing experiments but the two-state Landau-Zener model fails. The rate of change of the magnetic-flux density $|dB_C/dt|$ was assumed to be constant between the two inhomogeneous fields A and B. Magnetic-field simulations showed that especially for $\Delta B_C > 0.5$ T this is not exactly the case: The magnetic-flux density drops with a steep slope in the beginning of magnet C, varies hardly in the middle, and increases with a steep slope shortly before magnet B. The result is that the value of $|dB_C/dt|$ is larger than its mean value for most of the level crossings. Thus, the probability for an avoided crossing being traversed adiabatically should be even smaller which would result in a higher refocusing efficiency. Therefore, calculations with the two-state Landau-Zener model taking the actual magnetic-flux density into account would differ even more from the experimental observations. However, the change of the magnetic-flux density with time dB_C/dt is not easy to evaluate. In particular, the borders where magnets A, B, and C are connected are very delicate to treat and small misalignments may cause large local-field variations leading to unpredictable results. Furthermore, one needs to keep in mind that in many level systems interference of states occurs and the transition probabilities might be only approximately accessible by the two-state case when spin-rotation coupling is much smaller than the level separation. For the general case, transition probabilities cannot be calculated analytically [38,39]. In order to account for path interference one could numerically solve the multistate Landau-Zener problem to calculate transition probabilities. Diagonalizing the according $N \times N$ matrix with N being the total number of energy levels, one would directly get the transition amplitudes $S_{nn'}$ of state n for the system starting in state n'. Nevertheless, the large uncertainty in dB/dt on the molecular-beam path which enters Eq. (5) for the transition probability in the exponent will still be problematic in these calculations.

Some earlier works on the magnetic refocusing of molecules gave different explanations for their observation of incomplete refocusing. Amirav and Navon carried out magnetic deflection and refocusing experiments on organic molecules such as TEMPO [1,2]. They observed a reduced refocusing efficiency compared to the expectations derived from atomlike Stern-Gerlach behavior. Intramolecular spin relaxation with a defined spin-relaxation time τ was postulated. In the experiments on $Mn@Sn_{12}$ the refocusing efficiency varies dramatically with magnetic-field changes at constant transit time through the magnet arrangement. Therefore, spin-relaxation mechanisms with constant relaxation times can be ruled out.

In the discussion of the refocusing experiment it is generally assumed that no spin flips occur inside the inhomogeneous fields A and B. This assumption is rationalized primarily with the observation of a splitting in $2J + 1$ beam components in the Stern-Gerlach experiment for $Mn@Sn_{12}$. The vast majority of clusters of different sizes and compositions do not show this behavior even at our lowest possible nozzle temperatures. In most cases, a paramagneticlike, uniform deflection in gradient direction was observed. For pure transition-metal clusters, this observation can also be explained within the avoided-crossing model [24]. Nevertheless, a more detailed look into the dependence of rotational temperature and vibrational excitation is necessary for a thorough understanding of magnetic deflection experiments. Detailed work on lanthanide-doped tin clusters considering vibrational excitation is in preparation.

VI. CONCLUSION

We used magnetic double deflection experiments to show that the equidistant splitting in the Stern-Gerlach experiment

on cold, superatomic $Mn@Sn_{12}$ at low temperatures ($T_{nozzle} = 16$ K) can be reversed. In contrast to atomic beams, the change of the magnetic-flux density ΔB_C between the two deflection magnets turned out to have a tremendous effect on the refocusing efficiency η_{refoc} of this cluster: Minimizing ΔB_C to about 0.1 T we achieve $\eta_{refoc} = 90\%$ while larger flux density variations reduce the refocusing to about 30%. A microscopic model based on the coupling of rotational and spin degrees of freedom was used to explain the experimentally observed dependence of η_{refoc} on ΔB_C. It becomes clear that the two-state Landau-Zener model fails to explain the spin dynamics for the multilevel system within our model. Instead, assuming that a constant value of (1.0–1.5)% of all avoided level crossings are traversed adiabatically gives a satisfactory agreement with the experimental data. The failure of the two-state Landau-Zener model might be due to the multistate character of the studied system and is left open for further investigations.

ACKNOWLEDGMENTS

We want to thank A. Shayeghi for helpful discussions and H. de Gersem for access to magnetic-field simulation tools (CST Studio Suite). Furthermore we want to thank D. Schnur for help with the experimental work. We gratefully acknowledge the financial support of the Deutsche Forschungsgemeinschaft (DFG) through Grant No. SCHA 885/16-1. One of us (T.M.F.) wants to thank the "Merck'sche Gesellschaft für Kunst und Wissenschaft e.V." for a scholarship.

APPENDIX A: ASYMMETRY OF REFOCUSING BEAM PROFILES

The small asymmetry of the molecular-beam profiles that was observed in the refocusing experiments is discussed in more detail here. Analyzing the beam profiles shows a few percent more intensity into the opposite direction of the field gradient of the first Stern-Gerlach magnet A (negative z direction in Fig. 2). This observation can be rationalized within the avoided-crossing theory. Clusters in states with $dE/dB < 0$ are deflected in the gradient direction in magnet A. When R is small or $|R_z|$ is near R, the density of states with $dE/dB > 0$ that cross with the initial state under total angular momentum conservation is smaller than for states with $dE/dB < 0$. Thus, on average M_J should change only by a small amount and refocusing is more likely. On the other hand, clusters with $dE/dB > 0$ are deflected antiparallel to the gradient in magnet A. In this case the described effect is much smaller, M_J^B varies more from M_J^A, and refocusing is less efficient. Indeed, the calculated beam profiles are slightly asymmetric against gradient direction in magnet A. However, adiabatic level crossings during the field entrance increase the amount of clusters with $dE/dB < 0$ in magnet A. Thus, more clusters are deflected in the gradient direction in magnet A. Due to the higher refocusing probability for clusters in these states, the two effects partially cancel and asymmetry is reduced. In order to further study the asymmetry of the beam profiles of Stern-Gerlach as well as refocusing experiments, one has to repeat these with better cluster beam stability several times for better statistics.

APPENDIX B: FIELD ENTRANCE

In the literature, the field entrance into magnetic and electric fields has been mostly assumed to be of pure adiabatic character. This has usually been justified by the fact that clusters rotate on a time scale of $\tau_{rot} < 1$ ns whereas the field entrance is much slower (a few microseconds) [40,41]. This adiabatic behavior leads to an imbalance in the population of the $2J + 1$ spin states after field entrance because the coupled, adiabatic paths through the rotation-Zeeman diagram on average have a negative slope [24,27]. This is because there is a lower bound for the rotational energy ($R = 0$) but no upper bound and thus the density of states with $dE/dB < 0$ is larger than for states with $dE/dB > 0$ because they originate from higher energies at zero field. More precisely, below the energy level with $M_J = J$ and $R = |J_z^{tot} - M_J|$, no avoided level crossings of states with total angular moment in the z direction J_z^{tot} and $M_J = J$ can occur because of angular momentum conservation and $|R_z| \leqslant R$ [33]. This is shown for example by the bold, blue line in Fig. 3 for $J_z^{tot} = 32.5$ and $J = 2.5$. Consequently, the probability for a level crossing with an energy state for which $dE/dB < 0$ is increased which leads to an effective negative slope of the adiabatic path. This effect becomes more important with increasing electronic spin angular momentum J and is therefore much larger for pure transition-metal clusters than for clusters with only one magnetic atom.

In order to figure out the influence of the field entrance on the population of the $2J + 1$ spin states, i.e., if the passage of avoided level crossings modifies its distribution, the spin-state population during field entrance was calculated for the pure adiabatic ($p_{ad} = 1$), the pure diabatic case ($p_{ad} = 0$), and

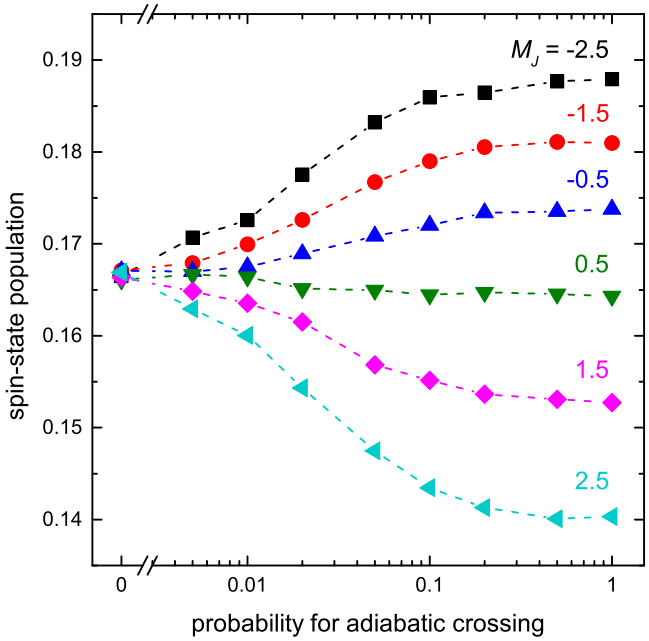

FIG. 8. Distribution of the spin state M_J for $Mn@Sn_{12}$ (spherical rotor, $J = S = 5/2$, $B_{rot} = 0.2$ m^{-1}) after entrance into a magnetic field with $B = 1.3$ T for different transition probabilities at avoided crossings in the rotation-Zeeman diagram. The rotational temperature is set to 10 K.

for some values in between by explicitly going through the rotation-Zeeman diagram from $B = 0$ to 1.3 T (analogous to Fig. 4) taking all avoided level crossings into account (Fig. 8). For the pure adiabatic case of $Mn@Sn_{12}$, the spin states with lowest and highest M_J have a relative population of 0.19 and 0.14, respectively. This difference should be observable in Stern-Gerlach experiments looking at the intensity of the $2J + 1$ beamlets: The beam components deflected in the gradient direction should be slightly enhanced. This effect is partially blurred by the known defocusing (focusing) effect in (against) the gradient direction [3,26]. A closer inspection of the experimental Stern-Gerlach beam profiles indeed reveals a slight asymmetry of a few percent [26] but the accuracy of the beam profile intensities, especially in the outer beam regions, is not sufficient to determine a value for p_{ad} by comparison with the calculation results in Fig. 8. However, all calculations shown in Fig. 5 were repeated applying both diabatic and adiabatic field entrance and no significant deviations were found.

[1] A. Amirav and G. Navon, Phys. Rev. Lett. **47**, 906 (1981).
[2] A. Amirav and G. Navon, Chem. Phys. **82**, 253 (1983).
[3] W. D. Knight, R. Monot, E. R. Dietz, and A. R. George, Phys. Rev. Lett. **40**, 1324 (1978).
[4] W. D. Knight, Helv. Phys. Acta **56**, 521 (1983).
[5] W. A. de Heer, P. Milani, and A. Châtelain, Phys. Rev. Lett. **65**, 488 (1990).
[6] W. A. de Heer, P. Milani, and A. Châtelain, Z. Phys. D **19**, 241 (1991).
[7] P. Ballone, P. Milani, and W. A. de Heer, Phys. Rev. B **44**, 10350 (1991).
[8] J. P. Bucher, D. C. Douglass, and L. A. Bloomfield, Phys. Rev. Lett. **66**, 3052 (1991).
[9] J. P. Bucher, D. C. Douglass, P. Xia, B. Haynes, and L. A. Bloomfield, Z. Phys. D **19**, 251 (1991).
[10] J. A. Becker and W. A. de Heer, Ber. Bunsen-Ges. Phys. Chem. **96**, 1237 (1992).
[11] J. G. Louderbeck, A. J. Cox, L. J. Lising, D. C. Douglass, and L. A. Bloomfield, Z. Phys. D **26**, 301 (1993).
[12] D. C. Douglass, A. J. Cox, J. P. Bucher, and L. A. Bloomfield, Phys. Rev. B **47**, 12874 (1993).
[13] I. M. L. Billas, J. A. Becker, A. Châtelain, and W. A. de Heer, Phys. Rev. Lett. **71**, 4067 (1993).
[14] I. M. L. Billas, J. A. Becker, and W. A. de Heer, Z. Phys. D **26**, 325 (1993).
[15] I. M. L. Billas, A. Châtelain, and W. A. de Heer, Science **265**, 1682 (1994).
[16] S. E. Apsel, J. W. Emmert, J. Deng, and L. A. Bloomfield, Phys. Rev. Lett. **76**, 1441 (1996).
[17] A. Hirt, D. Gerion, I. M. L. Billas, A. Châtelain, and W. A. de Heer, Z. Phys. D **40**, 160 (1997).
[18] I. M. L. Billas, A. Châtelain, and W. A. de Heer, J. Magn. Magn. Mater. **168**, 64 (1997).
[19] A. Châtelain, Philos. Mag. B **79**, 1367 (1999).
[20] D. Gerion, A. Hirt, I. M. L. Billas, A. Châtelain, and W. A. de Heer, Phys. Rev. B **62**, 7491 (2000).
[21] X. Xu, S. Yin, R. Moro, and W. A. de Heer, Phys. Rev. Lett. **95**, 237209 (2005).
[22] M. B. Knickelbein, J. Chem. Phys. **125**, 044308 (2006).
[23] F. W. Payne, W. Jiang, J. W. Emmert, J. Deng, and L. A. Bloomfield, Phys. Rev. B **75**, 094431 (2007).
[24] X. Xu, S. Yin, R. Moro, and W. A. de Heer, Phys. Rev. B **78**, 054430 (2008).
[25] X. Xu, S. Yin, R. Moro, A. Liang, J. Bowlan, and W. A. de Heer, Phys. Rev. Lett. **107**, 057203 (2011).
[26] U. Rohrmann and R. Schäfer, Phys. Rev. Lett. **111**, 133401 (2013).
[27] U. Rohrmann, P. Schwerdtfeger, and R. Schäfer, Phys. Chem. Chem. Phys. **16**, 23952 (2014).
[28] U. Rohrmann and R. Schäfer, J. Phys. Chem. C **119**, 10958 (2015).
[29] I. I. Rabi, S. Millman, P. Kusch, and J. R. Zacharias, Phys. Rev. **55**, 526 (1939).
[30] U. Rohrmann, S. Schäfer, and R. Schäfer, J. Phys. Chem. A **113**, 12115 (2009).
[31] B. A. Collings, A. H. Amrein, D. M. Rayner, and P. A. Hackett, J. Chem. Phys. **99**, 4174 (1993).
[32] J. B. Hopkins, P. R. R. Langridge-Smith, M. D. Morse, and R. E. Smalley, J. Chem. Phys. **78**, 1627 (1983).
[33] U. Rohrmann, Ph.D. thesis, Technische Universität Darmstadt 2014.
[34] I. I. Rabi, J. M. B. Kellogg, and J. R. Zacharias, Phys. Rev. **46**, 157 (1934).
[35] R. S. Title and K. F. Smith, Philos. Mag. **5**, 1281 (1960).
[36] C. Zener, Proc. R. Soc. London, Ser. A **137**, 696 (1932).
[37] R. Frisch and E. Segre, Z. Phys. **80**, 610 (1933).
[38] A. V. Shytov, Phys. Rev. A **70**, 052708 (2004).
[39] R. K. Malla and M. E. Raikh, Phys. Rev. B **96**, 115437 (2017).
[40] P. Dugourd, R. Antoine, M. Abd El Rahim, D. Rayane, M. Broyer, and F. Calvo, Chem. Phys. Lett. **423**, 13 (2006).
[41] S. Heiles, S. Schäfer, and R. Schäfer, J. Chem. Phys. **135**, 034303 (2011).